SSRG International Journal of Electrical and Electronics Engineering
ISSN: 2348-8379/ https://doi.org/10.14445/23488379/IJEEE-V10I8P101

Volume 10 Issue 8, 1-8, August 2023

Original Article

Piezoelectric-Based Square Diaphragm Pressure Sensor Modelling and Analysis using PZT-5H and PZT-5A

Moirangthem Shamjit Singh[1], Pradip Kumar Kalita[2], Maibam Sanju Meetei[3]

[1,2]*Department of Physics, Rajiv Gandhi University, Arunachal Pradesh, India.*
[3]*Department of Electronics and Communication Engineering, Rajiv Gandhi University, Arunachal Pradesh, India.*

[3]*Corresponding Author : maibamkhuman@gmail.com*

Received: 01 June 2023 Revised: 05 July 2023 Accepted: 02 August 2023 Published: 31 August 2023

Abstract *- This study presents the analytical model and 3D model simulation of the piezoelectric square diaphragm pressure based on PZT-5H and PZT-5A. The sensor's pressure stress model and electrostatic model are explained in the analytical model of the sensor, and all the variables impacting the induced stress and output voltage are covered. Piezoelectric materials such as PZT-5A, PZT-5H and PZT-5J, PVDF, PMN-PT, $LiNbO_3$, AlN, and ZnO are used to create pressure sensors. The COMSOL Multiphysics simulator simulates the suggested 3D sensor model to verify the analytical model. The validation of the analytical model using the simulated values revealed that the sensor's output characteristics are linear with applied pressure and have a negative slope. This study also identifies the negative voltage that forms when tensile stress occurs. The analytical and simulated values of the PZT-5H-based sensor's sensitivities are -5.879 mV/kPa and -6.279 mV/kPa, respectively. The analytical and simulated values for the PZT-5A-based sensor's sensitivities are -7.468 mV/kPa and -7.347 mV/kPa, respectively.*

Keywords *- Equivalent circuit, Linear, Natural plane, Voltage coefficient, Sensitivity.*

1. Introduction

With the Internet of Things (IoT) development, exceptionally accurate and robust sensors have become essential in today's technological environment. The pressure sensor is one of the most commonly used among the different types of sensors. Piezoelectric-based pressure sensors are the most versatile and often used to detect pressure in various applications like industries, medicine, motor vehicles, IoT, energy harvesting, etcetera [1]. Piezoelectric pressure sensors have received much attention due to their excellent linearity, high sensitivity, ease of integration with other components, versatility, and lightweight. This piezoelectric pressure sensor has unique characteristics that enable sensitivity, accuracy, adaptability, and durability by translating mechanical pressure into electrical signals [2].

A piezoelectric material undergoes internal structural change due to mechanical pressure or stress, such as compression or bending, according to the fundamental operating principle of a piezoelectric pressure sensor. The deformation results in a new distribution of charged particles; the produced charges become polarised, which generates an electric potential throughout the material. It is known as the direct piezoelectric effect. On the other hand, when an electric field is applied, a piezoelectric material deforms mechanically because of the shifting of the charged particles inside the material. It is known as the reverse piezoelectric effect. As a result, the piezoelectric action is also reversible [3]. A variety of different piezoelectric materials were used to build the pressure sensor.

The commonly used piezoelectric by the researcher for developing pressure sensors are Lithium Niobate ($LiNbO_3$), Quartz, Lead Magnesium Niobate-Lead Titanate (PMN-PT), Polyvinylidene Fluoride (PVDF), Aluminium Nitride (AlN), Lead Zirconate Titanate (PZT) and Zinc Oxide (ZnO) [4-7]. One of the most popular and best piezoelectric materials is PZT, which is also utilised in piezoelectric pressure sensors. Additionally, PZTs have a high piezoelectric voltage coefficient and are employed in applications that need durability. A material's piezoelectric coupling coefficient, which is high in PZT, determines its capacity to transform mechanical energy into electrical energy and vice versa. It also shows superior mechanical and electrical qualities[8-10]. PZT is a ceramic material employed in environments with high temperatures for pressure sensors [11].

PZT comes in various forms, but PZT-5H and PZT-5A are the two most frequently used in manufacturing; thus, in this study, we are considering these two PZTs in this investigation.

2. Sensor Model and Equivalent Circuit

2.1. Sensor Structure

Figure 1 depicts the basic cross-sectional layout of the piezoelectric pressure sensor with a square diaphragm. In this study, piezoelectric sensing materials PZT-5H and PZT-5A are used. Silicon (Si) functions as the sensor's mechanical structure and is used as its substrate. Silicon Dioxide (SiO2), which functions as an insulator, keeps the substrate body and electrode apart[12]. Gold (Au), which acts as the electrodes for the sensor, is coated on the top and bottom surfaces of the piezoelectric sensing material.

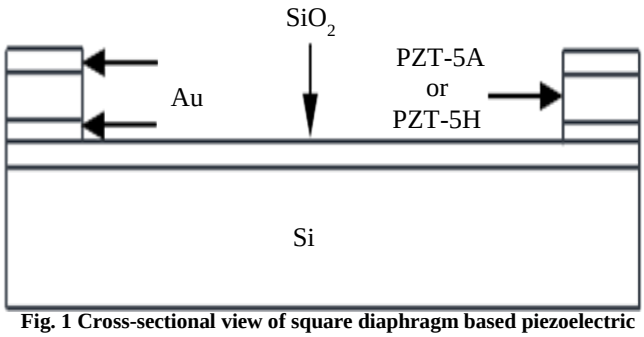

Fig. 1 Cross-sectional view of square diaphragm based piezoelectric pressure sensor

2.2. Equivalent Circuit Model

Because of the pressure or force being applied, the piezoelectric material within the piezoelectric sensor deforms under stress. Charges (Q_{Piezo}) are generated due to this deformation and accumulate on the piezoelectric surfaces' opposing sides. The opposite sides of the piezoelectric material encountered compressive stress on one side and tensile stress on the other. As a result, the opposite charge formed between the two surfaces and the device behaved like a capacitor (C_{Piezo}). The sensor's output is a potential difference (V_{Piezo}) produced between the two surfaces by the opposing charges. Figure 2 illustrates the equivalent circuit schematic.

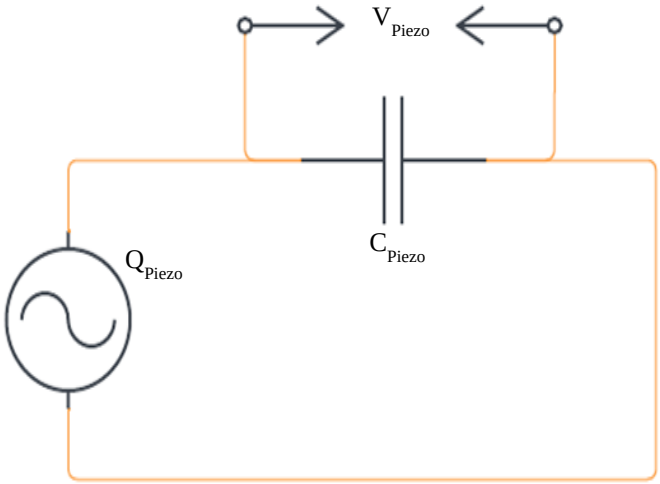

Fig. 2 Piezoelectric sensor equivalent circuit diagram

3. Analytical Model

To convert input pressure to output voltage in this study, a piezoelectric sensor model is used for analyses. Stress is created on the sensor's surface due to pressure applied to the sensor's diaphragm.

The surface of the piezoelectric material generates charges, and the piezoelectric material behaves like a capacitor. The potential gradient between the two surfaces is the sensor's output voltage. Therefore, the sensor's pressure stress and electrostatic models are crucial to understand.

3.1. Pressure-Stress Model

In this study, let's consider a rectangular diaphragm-structured piezoelectric pressure sensor. The input Pressure (P) causes deflection ($w(x,y)$) and stress ($T(x,y)$) in the rectangular diaphragm when it is applied to its surface with a fixed edge at $x=a$ and $y=b$ and the value of $x=y=0$ in the middle. The diaphragm's deflection equation is mathematically presented as follows in [13-15]:

$$w(x,y) = k(a^2 - x^2)^2(b^2 - y^2)^2 \tag{1}$$

Where k = constant, and it can be express as:

$$k = \frac{7P}{128D\left(a^4+b^4+\frac{4}{7}a^2b^2\right)} \tag{2}$$

Where D = flexure rigidity, and it can be express as:

$$D = \frac{Eh^3}{12(1-\nu^2)} \tag{3}$$

Where E = Young's modulus, ν = Poisson's ratio, and h = thickness of the diaphragm.

Let us look at equations 1 and 2 for a square diaphragm. By putting the values for a = b into equations 1 and 2, we can write these equations as follows.

$$w(x,y) = k(a^2 - x^2)^2(a^2 - y^2)^2 \tag{4}$$

$$k = \frac{0.02127P}{Da^4} \tag{5}$$

There are two types of stress, standard stress component and shear stress; the two everyday stresses are along the x-direction (T_{xx}) and y-direction (T_{yy}). The shear stress (T_{xy}) is stress-induced along the z-direction. The mathematical expression of these stresses is as follows [11-14]:

$$T_{xx} = \frac{Ez}{1-\nu^2}\left(\frac{\partial^2 w}{\partial x^2} + \nu\frac{\partial^2 w}{\partial y^2}\right) \tag{6}$$

$$T_{yy} = \frac{Ez}{1-\nu^2}\left(\frac{\partial^2 w}{\partial y^2} + \nu\frac{\partial^2 w}{\partial x^2}\right) \tag{7}$$

$$T_{xy} = \frac{Ez}{1-v^2}\left(\frac{\partial^2 w}{\partial x \partial y}\right) \quad (8)$$

Where z = is the distance from the natural plane. For a homogenous material diaphragm, the value of z is half of the thickness of the diaphragm. Now, the stress equation can be written as follows:

$$T_{xx} = -1.02P\frac{za^2}{h^3}\left[\left(1-\left(\frac{y}{a}\right)^2\right)^2\left(1-3\left(\frac{x}{a}\right)^2\right)^2 + v\left(1-\left(\frac{x}{a}\right)^2\right)^2\left(1-3\left(\frac{y}{a}\right)^2\right)^2\right] \quad (9)$$

$$T_{yy} = -1.02P\frac{za^2}{h^3}\left[\left(1-\left(\frac{x}{a}\right)^2\right)^2\left(1-3\left(\frac{y}{a}\right)^2\right)^2 + v\left(1-\left(\frac{y}{a}\right)^2\right)^2\left(1-3\left(\frac{x}{a}\right)^2\right)^2\right] \quad (10)$$

$$T_{xy} = 4.09P\frac{za^2}{h^3}(1-v)\left(1-\left(\frac{x}{a}\right)^2\right)\left(1-\left(\frac{y}{a}\right)^2\right)\frac{xy}{a^2} \quad (11)$$

Now, let us find out the maximum everyday stresses along the x-direction and y-direction, as these stresses are directly proportional to the output voltages of the piezoelectric. The maximum stress occurs at the center of the edges, i.e. $x = a$ and $y = 0$ or $y = a$ and $x = 0$. Now, the maximum stress equation can be written as follows:

For $x = a$ and $y = 0$, the stress equation 9 can be written as follow:

$$T_{xx} = 2.04P\frac{za^2}{h^3} \quad (12)$$

For $x = 0$ and $y = a$, the stress equation 10 can also be written as:

$$T_{yy} = 2.04P\frac{za^2}{h^3} \quad (13)$$

The maximum stress occurs at the middle of the edges in both the x-direction and y-directions, according to equations 10 and 11 above. The z, a, and h values also affect the sensor's maximum stress.

3.2. Electrostatic Model

According to the equivalent circuit concept depicted in Figure 2, as charge accumulates on the piezoelectric material's surface, it acts like a capacitor by creating a potential difference between the surfaces.

$$V = \frac{Q}{C} \quad (14)$$

C = capacitance between the two electrodes, Q = charges generated, and V = the sensor's output voltage.

Since it is widely known that the top surface's edges generate the maximum tensile stress and that pressure-induced stress also directly correlates to generating charges; for maximum output voltage generation, the piezoelectric material is fastened close to the margins of the diaphragm.

The electrostatic charge generated by the induced stress on the piezoelectric material's surface is described as follows [16, 17]:

$$q(x) = T_{xx}d_{31} \quad (15)$$

Where $q(r)$ = generated charge on the surface and d_{31} = piezoelectric strain constant.

Now consider a piezoelectric material of square form positioned on a square diaphragm with length l. The total charge generated on the surface is $Q(x)$ on the square surface and is denoted by:

$$Q(x) = l^2 T_{xx}(x)d_{31} \quad (16)$$

For a square plate, the capacitance is given by:

$$C = \frac{\epsilon_{33}l^2}{t} \quad (17)$$

Where t = piezoelectric thickness and ε_{33} = permittivity of the piezoelectric material.

From Equation 16 and Equation 17, the output voltage of the piezoelectric pressure sensor can be rewritten as:

$$V(x) = \frac{tT_x(x)d_{31}}{\epsilon_{33}} \quad (18)$$

Again, the equation 18 can be rewritten as:

$$V(x) = tT_x(x)g_{31} \quad (19)$$

Since the value of g_{31} is given by:

$$g_{31} = \frac{d_{31}}{\epsilon_{33}} \quad (20)$$

The piezoelectric material's thickness, the amount of stress-induced on the surface, and the voltage coefficient of the piezoelectric are all directly related to the sensor's output voltage.

3.3. Sensitivity

The device's sensitivity is defined as the ratio of output signal magnitude changes to input signal magnitude changes. The following equation can be used to represent the Sensitivity (S):

$$S = \frac{V_n - V_m}{P_n - P_m} \quad (21)$$

Where the sensor output voltage V_m and V_n are for the applied pressure of P_n and $P_{m,}$ respectively.

4. Results and Discussion

The modelled sensor can be manufactured or simulated using a Finite Element Method simulator (FEM) to test the theoretical model. FEM is widely used to examine how different design parameters affect sensor performance fast and precisely. This study uses COMSOL Multiphysics 5.2® is used to model the sensor and validate the theoretically calculated piezoelectric sensor.

4.1. Diaphragm Structure Design

To increase sensitivity, the diaphragm area should be as large as possible, and the thickness should be as little as possible [18]. However, more extensive and thinner diaphragms result in more nonlinearity and structural stress, which can cause issues with reliability.

The side length and thickness of the diaphragm should be less than 3500 μm and more significant than 20 μm, respectively, considering the problems mentioned above and the present process capacity.

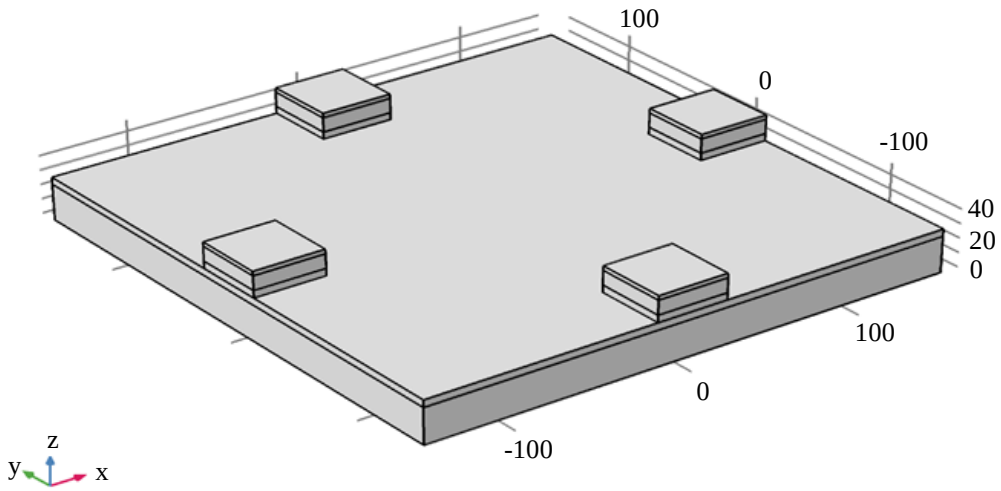

Fig. 3 The sensor's 3D model in the COMSOL multiphysics simulator

Table 1. Specifications of the materials used to design the sensor

Types of Material	Poisson's Ratio	Young's Modulus	Piezoelectric Voltage Coefficient
PZT-5H	0.31	50 GPa	-9.5×10^{-3} Vm/N
PZT-5A	0.34	52 GPa	-11.3×10^{-3} Vm/N
SiO_2	0.17	70 GPa	-
Si	0.22	160 GPa	-
Au	0.44	70 GPa	-

Figure 3 shows a 3D representation of the proposed sensor's structure in the COMSOL multiphysics simulator. The most widely used diaphragm dimension is a square silicon (Si) diaphragm with a length of 300 μm and a thickness of 25 μm.

A Silicon Dioxide (SiO_2) insulator with a thickness of 5 μm is placed on top of the silicon substrate. Gold (Au) electrodes with a thickness of 5 μm is affixed to the top and bottom of the piezoelectric sensing material made of PZTs. On top of the surface, the input pressures are applied. Table 1 lists the material characteristics that were used in the simulation.

4.2. Initial and Boundary Conditions

Choosing the suitable Physics modules and setting the different settings before starting the simulation is essential. This approach employs piezoelectric modules as an intermediary between the two physics of electrostatics and solid mechanics. The 3D model of the sensor is designed in the COMSOL, and the material is assigned to the relevant components in the COMSOL 3D model structure. After the physics setup is completed, the meshing with the finer tetrahedral shape is carried out. Compute the study of the modelled sensor in the simulator for the applied pressure range of 0 to 100 kPa with a step size of 10 kPa once the mesh has been generated.

4.3. Model Validation

Based on the suggested model of the sensor, whose characteristics and dimensions are provided in the preceding section, simulation analysis using COMSOL Multiphysics is carried out to validate the analytical model. Simulation is done, and varied outputs are seen for the applied pressure range of 0-100 kPa. The simulated-output stress distribution at an input pressure of 100 kPa is shown in Figure 4 for the sensor's surface. The sensor model equation demonstrates that a symmetrical stress is generated on a square diaphragm building's surface and that the maximum stress is generated at the centre of the sensor's edges, which is also demonstrated in the output of the stress distribution. Additionally, tensile stress on the surface is seen to be the output stress.

The distribution of the predicted output voltage at a 100 kPa input pressure applied to the sensor's surface is shown in Figures 5 and 6. The sensor exhibits a more excellent output voltage value when it is near the mid of the edges of the top layer. It was also observed that a negative output voltage occurred on the piezoelectric material's top surface.

Figures 4, 5 and 6 show that a negative voltage is generated where the tensile stress has occurred. It also observed that the PZT-5A-based piezoelectric pressure has a higher output voltage than the PZT-5H-based pressure sensor. This is because of the higher values of piezoelectric voltage coefficient for PZT-5A piezoelectric material than the PZT-5H piezoelectric material.

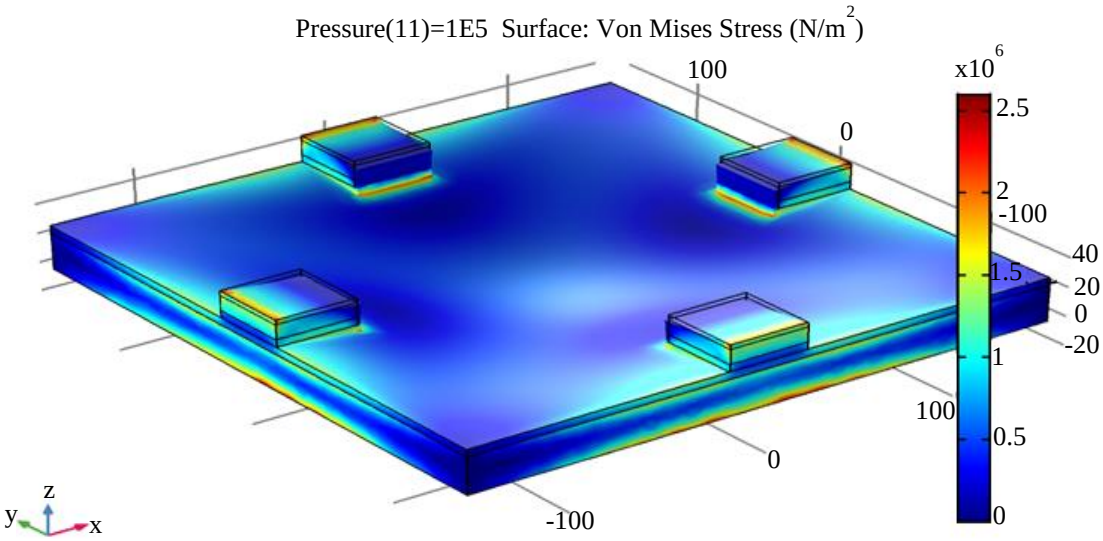

Fig. 4 Distribution of simulated output stress of the sensor for the 100 kPa applied pressure

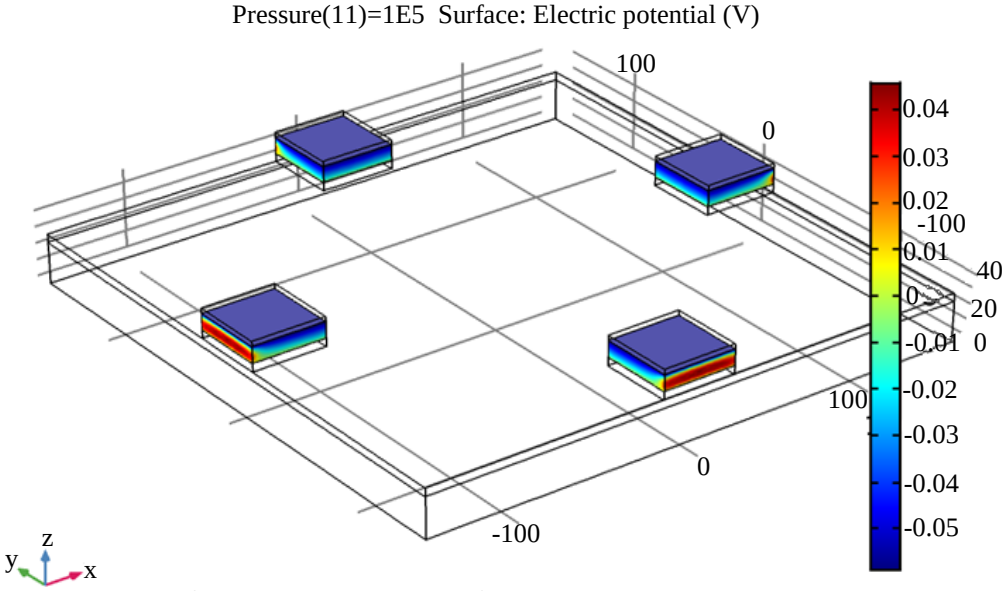

Fig. 5 Distribution of the simulated output voltage of the PZT-5H-based sensor under a 100 kPa applied pressure

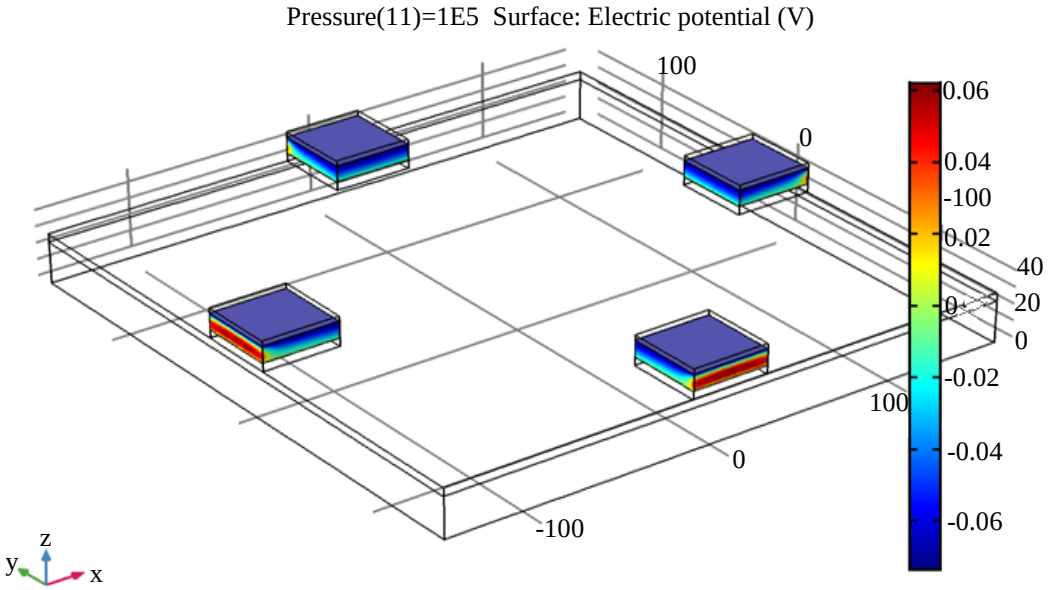

Fig. 6 Distribution of the simulated output voltage of the PZT-5A-based sensor under a 100 kPa applied pressure

Figures 7 and 8 display the sensor's simulated output voltage and the applied pressure ranges of 0 to 100 kPa. Again, it is demonstrated that the output voltage rises in magnitude but with negative values as the applied pressure increases.

It indicates a linear relationship with a negative slope between the output of the pressure sensor and the applied pressure. The output voltages are in the millivolt range for the applied pressure in kPa. The model equation for the sensor also exhibits the simulated output characteristic. Table 2 illustrate the comparative output voltage of the simulated and analytical values for the proposed PZT-5H and PZT-5A piezoelectric-based square diaphragm pressure sensor. It can be seen that the analytical values and the simulated output values are relatively close to one another. A further observation is that the size of the analytical and simulated quantities rises with rising in the input pressure but with a negative slope. The analytical model that has been proposed is valid, as shown by this comparison of the sensor model's analytical and simulated performance.

From Table 2, the sensitivity of the simulated and analytical values of the PZT-5H-based sensor is -5.879 mV/kPa and -6.279 mV/kPa, respectively. Moreover, the sensitivity of the simulated and analytical values for the PZT-5A-based sensor is -7.347 mV/kPa and -7.468 mV/kPa, respectively.

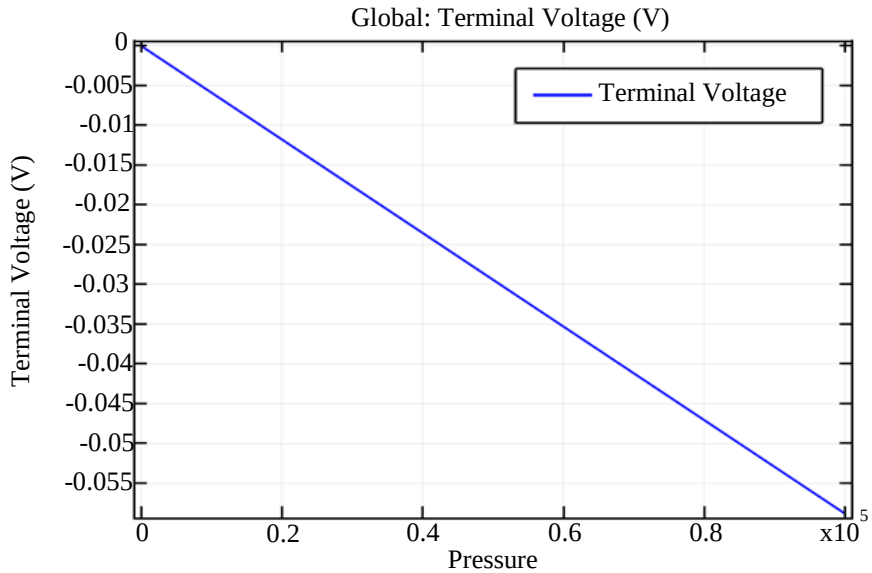

Fig. 7 Graph illustrates the simulated output voltage for the pressure range of 0 to 100 kPa for the PZT-5H-based pressure sensor

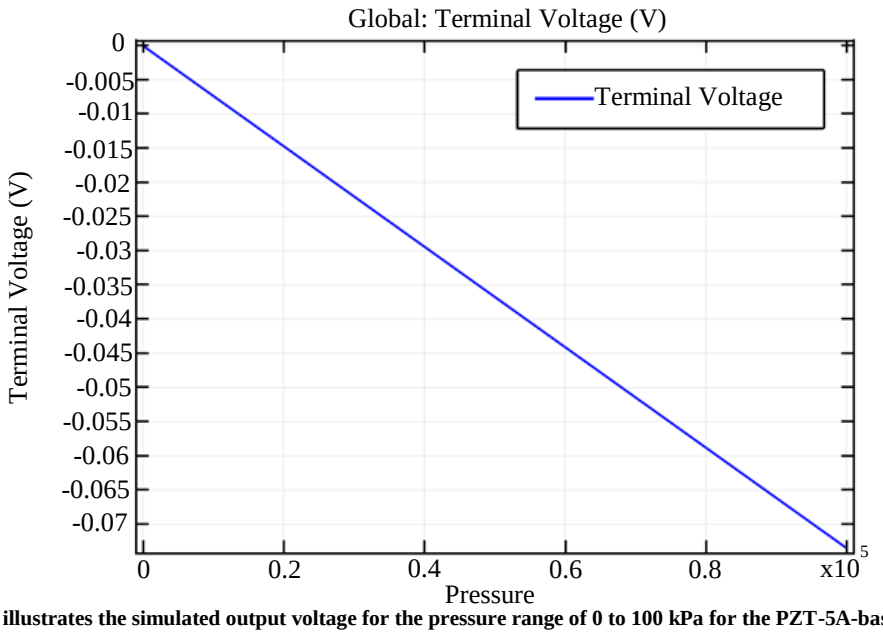

Fig. 8 Graph illustrates the simulated output voltage for the pressure range of 0 to 100 kPa for the PZT-5A-based pressure sensor

Table 2. Simulated and calculated output voltage of the sensor

Applied Pressure [kPa]	PZT-5H-based Piezoelectric Pressure Sensor		PZT-5A-based Piezoelectric Pressure Sensor	
	Simulated	Calculated	Simulated	Calculated
0	0	0	0	0
10	-5.879	-6.279	-7.347	-7.468
20	-11.759	-12.558	-14.694	-14.937
30	-17.639	-18.837	-22.042	-22.406
40	-23.518	-25.116	-29.389	-29.875
50	-29.398	-31.395	-36.737	-37.344
60	-35.278	-37.674	-44.084	-44.813
70	-41.157	-43.953	-51.432	-52.281
80	-47.037	-50.233	-58.779	-59.750
90	-52.917	-56.512	-66.127	-67.219
100	-58.796	-62.791	-73.474	-74.688

5. Conclusion

The main objectives of this research study are the analytical modelling and simulation of the square diaphragm-based PZT-5H and PZT-5A piezoelectric pressure sensor for sensing 0-100 kPa and validation of the analytical model. An analytical model of the provided sensor is validated using the output data from the simulation of PZT-5H and PZT-5A.

The simulated and calculated results based on PZT-5A and PZT-5H are relatively near together, allowing for the proposed analytical model of the sensor to be applied in the future. The primary variables determining the sensor's output are the square diaphragm's length, height, distance from the natural plane, height of the piezoelectric material, and voltage coefficient. In areas where tensile stress has developed, it is discovered that the sensor output is negative. It is further noted that the output voltage for the proposed model exhibits linear magnitude variation with a negative slope. The analytical and simulated values of the PZT-5H-based sensor's sensitivities are -5.879 mV/kPa and -6.279 mV/kPa, respectively. The analytical and simulated values for the PZT-5A-based sensor's sensitivities are -7.468 mV/kPa and -7.347 mV/kPa, respectively.

Acknowledgments

The authors would like to thank the authority of Rajiv Gandhi University, Arunachal Pradesh, India, for the constant support and appreciation received while preparing the research work. All the authors contributed equally to this work.

References

[1] Tahera Kalsoom et al., "Advances in Sensor Technologies in the Era of Smart Factory and Industry 4.0," *Sensors*, vol. 20, no. 23, pp. 1-22, 2020. [CrossRef] [Google Scholar] [Publisher Link]

[2] Kenji Uchino, "Piezoelectric Devices for Sustainability Technologies," *Reference Module in Earth Systems and Environmental Sciences*, 2022. [CrossRef] [Google Scholar] [Publisher Link]

[3] N. Soin, S. C. Anand, and T. H. Shah, *12 - Energy Harvesting and Storage Textiles*, Handbook of Technical Textiles, 2nd ed., Woodhead Publishing, vol. 2, pp. 357-396, 2016. [CrossRef] [Google Scholar] [Publisher Link]

[4] Diego Galar, and Uday Kumar, *Actuators and Self-Maintenance Approaches*, eMaintenance Essential Electronic Tools for Efficiency, Academic Press, pp. 475-527, 2017. [CrossRef] [Publisher Link]

[5] Hao Wang, and Abbas Jasim, *Piezoelectric Energy Harvesting from Pavement*, Eco-Efficient Pavement Construction Materials, In Woodhead Publishing Series in Civil and Structural Engineering, pp. 367-382, 2020.[CrossRef] [Google Scholar] [Publisher Link]

[6] Abhinav V. Deshpande, "Energy Harvesting from Piezoelectric Material using Human Motion," *SSRG International Journal of VLSI & Signal Processing*, vol. 6, no. 2, pp. 5-8, 2019. [Google Scholar] [Publisher Link]

[7] Maibam Sanju Meetei, and Heisnam Shanjit Singh, "Design, Simulation and Optimization of PZT-5A Cantilever Piezoelectric Pressure Sensor," *Journal of Scientific Research and Reports*, vol. 29, no. 6, pp. 23-31, 2023. [CrossRef] [Google Scholar] [Publisher Link]

[8] Amal Megdich, Mohamed Habibi, and Luc Laperrière, "A Review on 3D Printed Piezoelectric Energy Harvesters: Materials, 3D Printing Techniques, and Applications," *Materials Today Communications*, vol. 35, p. 105541, 2023. [CrossRef] [Google Scholar] [Publisher Link]

[9] Maibam Sanju Meetei, Aheibam Dinamani Sihgh, and Swanirbhar Majumder, "A Novel Design Approach for Beam Bridge Structure Pressure Sensor Base on PZT-5A Piezoelectric," *Journal of Engineering Science and Technology Review*, vol. 14, no. 1, pp. 193-199, 2021. [CrossRef] [Google Scholar] [Publisher Link]

[10] Vladimír Kutiš et al., "MEMS Piezoelectric Pressure Sensor-Modelling and Simulation," *Procedia Engineering*, vol. 48, pp. 338-345, 2012. [CrossRef] [Google Scholar] [Publisher Link]

[11] Rob Carter, and Richard Kensley, Introduction to Piezoelctric Transducer. [Online]. Available: https://piezo.com/pages/intro-to-piezoelectricity

[12] Igor V. Linchevskyi, "Excitation of Surface Acoustic Waves in a Zsection of Piezoelectric Crystals by the Electric Field of a Long Electrode," *SSRG International Journal of Applied Physics*, vol. 6, no. 3, pp. 42-50, 2019. [CrossRef] [Google Scholar] [Publisher Link]

[13] S. Timoshenko, and S. Woinowsky-Krieger, *Theory of Plates and Shells*, 2nd ed., McGraw Hill Book Company, New York, 1959. [Google Scholar] [Publisher Link]

[14] Ansel C. Ugural, *Plates and Shells: Theory and Analysis*, 4th ed., CRC Press, Boca Raton, Florida, 2018. [Google Scholar] [Publisher Link]

[15] Minhang Bao, *Analysis and Design Principles of MEMS Devices*, 1st ed., Elsevier, 2005. [Google Scholar] [Publisher Link]

[16] Maibam Sanju Meetei et al., "A Novel Design and Optimization for Beam Bridge Piezoelectric Pressure Sensor," *International Journal of Advanced Research in Engineering and Technology*, vol. 11, no. 12, pp. 2687-2701, 2020. [CrossRef] [Google Scholar] [Publisher Link]

[17] Ingo Kuehne et al., "A New Approach for MEMS Power Generation Based on a Piezoelectric Diaphragm," *Sensors and Actuators A: Physical*, vol. 142, no. 1, pp. 292-297, 2008. [CrossRef] [Google Scholar] [Publisher Link]

[18] Mario Di Giovanni, *Flat and Corrugated Diaphragm Design Hand Book*, Marcel Dekker Inc., Newyork, 1982. [Google Scholar] [Publisher Link]